IEEE Photonics Journal
An IEEE Photonics Society Publication

All-Optical Signal Regeneration in Polarization-Division-Multiplexing Systems

Volume 3, Number 4, August 2011

A.-L. Yi, Student Member, IEEE
L.-S. Yan, Senior Member, IEEE
B. Luo, Member, IEEE
W. Pan, Member, IEEE
J. Ye, Student Member, IEEE

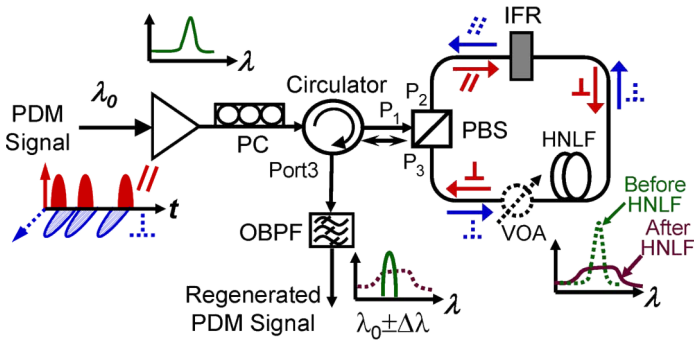

DOI: 10.1109/JPHOT.2011.2160937
1943-0655/$26.00 ©2011 IEEE

All-Optical Signal Regeneration in Polarization-Division-Multiplexing Systems

A.-L. Yi, *Student Member, IEEE*, L.-S. Yan, *Senior Member, IEEE*, B. Luo, *Member, IEEE*, W. Pan, *Member, IEEE*, and J. Ye, *Student Member, IEEE*

Center for Information Photonics and Communications, School of Information Science and Technology, Southwest Jiaotong University, Chengdu 610031, China

DOI: 10.1109/JPHOT.2011.2160937
1943-0655/$26.00 ©2011 IEEE

Manuscript received May 18, 2011; revised June 23, 2011; accepted June 24, 2011. Date of publication June 30, 2011; date of current version July 19, 2011. This work was supported by the National Natural Science Foundation of China (60972003), the Program for New Century Excellent Talents in University (NCET-08-0821), the Research Project in Sichuan Province of China (2010HH0009), and the State Key Laboratory of Advanced Optical Communication Systems and Networks of China. Corresponding author: L.-S. Yan (e-mail: lsyan@home.swjtu.edu.cn).

Abstract: Schemes of all-optical regeneration in polarization-division-multiplexing (PDM) systems are proposed and demonstrated with 2 × 10-Gb/s return-to-zero on–off-keying (RZ-OOK) transmission. Regeneration is achieved based on self-phase-modulation (SPM) effect and detuned filtering in highly nonlinear fiber (HNLF) with a polarization-diversified loop configuration. Furthermore, the ability of mitigating polarization-mode-dispersion (PMD) effects in PDM systems is evaluated. More than 3.7-dB eye-diagram-based signal-to-noise-ratio (SNR) improvement is achieved in the presence of 6.3-ps PMD as the pulsewidth of the PDM signal is about 18 ps.

Index Terms: All-optical regeneration, self-phase-modulation (SPM), polarization-division-multiplexing (PDM), highly nonlinear fiber, polarization mode dispersion.

1. Introduction

Driven by increasing demands on sustained traffic capacity with so many emerging techniques (e.g., IPTV, FTTX, etc.) that require large bandwidth, scientists and engineers are spending a lot of effort to find related solutions [1]. Among various approaches, polarization-division-multiplexing (PDM) is one of the enabling techniques that can double the system capacity directly by carrying two data channels on orthogonal polarization states but at the same wavelength [2], [3], and over the past few years, numerous PDM-based hero experiments have been demonstrated [4]–[6].

On the other hand, all-optical regeneration is a potential enabler for future all-optical networks [7]–[25], as it may simplify the network configuration without complicated and bit-rate dependent optical-electrical-optical (O-E-O) conversion. Many schemes of all-optical regeneration have been demonstrated based on different nonlinear mechanisms and different nonlinear media for various modulation formats. Among them, self-phase-modulation (SPM)-based all-optical regeneration using nonlinear optical fiber is a hot topic due to its simplicity, all-fiber nature, and bit-rate independence [13]–[21].

Currently and again, driven by the need of capacity, optical communication systems are becoming increasingly more complicated, including advanced modulation formats, dynamic wavelength manipulation, reconfigurable traffic, etc. Therefore, approaches have to take into account more dimensions (or degrees of freedom) of transmitted signals than ever before. For all-optical

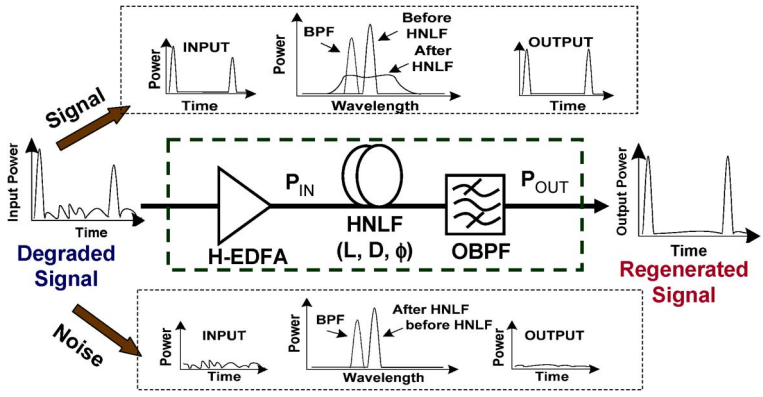

Fig. 1. Conceptual diagram of the single-channel SPM-based 2R regenerator. H-EDFA: high-power EDFA; OBPF: optical bandpass filter; HNLF: highly nonlinear fiber.

regeneration, it would be desirable to handle more channels simultaneously using only one module. Researchers have demonstrated all-optical regeneration (typically SPM-based) for multiple wavelengths [22]–[25]. Although other nonlinear signal processing functionalities (e.g., wavelength conversion) have been achieved for PDM signals [26]–[28], there are only a limited number of approaches of all-optical regeneration that can handle PDM signals using a single module [29].

In addition, polarization-mode-dispersion (PMD) is a much more severe challenge for PDM systems compared with standard single-polarization wavelength channels [30]–[32]. Approaches to overcome PMD-induced degradations in PDM systems include (i) electronic signal processing [33], (ii) dynamic polarization tracking followed by optical PMD compensators [34], and (iii) novel data formats, e.g., optical orthogonal frequency division multiplexing (OFDM), etc. [35].

From above, we can get an idea that it would be desirable to have an effective approach of all-optical regeneration for PDM signals even in the presence of PMD effects. In this paper, we propose an SPM-based all-optical regenerator through a nonlinear polarization-diversified loop for 2 $\times$ 10-Gb/s return-to-zero on–off-keying (RZ-OOK) PDM systems. The loop configuration can regenerate two polarization tributaries of the PDM signal simultaneously and reassemble the regenerated signals back to PDM signals automatically. In particular, we successfully demonstrate the ability of PMD mitigation based on the proposed scheme. Performances of regeneration and mitigation are given to illustrate its effectiveness.

The paper is structured as follows: The operation principle of proposed regenerator based on polarization-diversified loop is discussed in Section 2 with a typical experimental setup shown in Section 3. Experimental results about regeneration and PMD mitigation are given in Sections 4 and 5, respectively. The final section concludes our research.

2. Operation Principle

2.1. SPM-Based 2R Regeneration

First, we briefly recall the principle of the SPM-based Mamyshev single channel (one wavelength and one polarization) regenerator as shown schematically in Fig. 1. The degraded signal includes the signal itself (especially with different "1"-levels) and the noise part: (i) For the signal part, after the high-power EDFA (H-EDFA), it enters a given length of highly nonlinear fiber (HNLF) with a certain amount of chromatic dispersion. The signal spectrum will be significantly broadened and then a reshaped but clean spectrum can be obtained using a detuned optical bandpass filter (OBPF). (ii) The noise part can be mostly eliminated due to its broadband nature and through optical filtering.

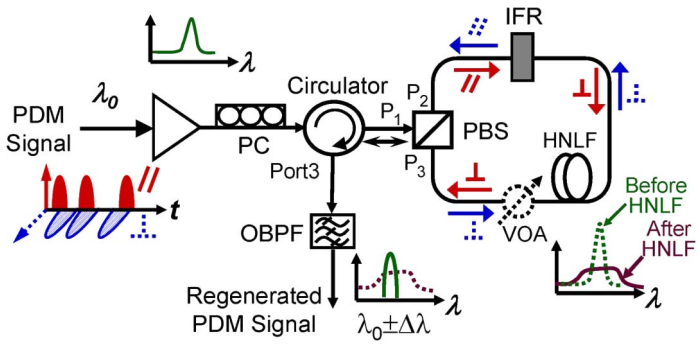

Fig. 2. Conceptual diagram of the proposed 2R regenerator for PDM signals. PC: polarization controller; IFR: in-line Faraday rotator; PBS: polarization beam splitter; VOA: variable optical attenuator.

2.2. PDM Regenerator

The conceptual diagram of the proposed all-optical PDM regenerator using the nonlinear polarization-diversified loop is shown in Fig. 2. Amplified and degraded PDM signals at the wavelength of λ_0 are demultiplexed by the polarization controller (PC) and the polarization beam splitter (PBS) and then counter-propagate through the nonlinear polarization-diversified loop. Based on the loop configuration, two orthogonal polarization components of PDM signals exhibit the same spectral broadening due to the SPM effect in the nonlinear medium (i.e., HNLF) under the pump of H-EDFA. Inside the loop, an in-line Faraday rotator (IFR) with a round-trip polarization rotation of 90° is used to automatically change the state of polarization (SOP) of the signals in both directions (a PC can also be used but may suffer from complicated and dynamically precise control). Therefore, two counter-propagating orthogonal polarization components are recombined at the input port of the PBS after traveling through the loop and then guided out of the loop by the circulator (Port 3). Finally, a single tunable OBPF is used to slice the broadened spectra of PDM signals at the wavelength of$\lambda_0 \pm \Delta\lambda$ to obtain the regenerated signals. Note that there are only one H-EDFA, one section of nonlinear medium and one OBPF for both orthogonal polarization components (i.e., a single regeneration module). A variable optical attenuator (VOA) may be required to balance the input power into the HNLF between two polarization tributaries. Compared with our previous scheme [29], the new approach is simplified: (i) fewer components (i.e., PBS, circulators, etc.); (ii) unnecessary polarization control inside the loop utilizing the IFR, although dynamic control is still required outside the loop.

3. Experimental Setup

To evaluate the regeneration performance and perform the PMD mitigation experiment, we build a typical setup, as shown in Fig. 3. It consists of a 2 × 10-Gb/s RZ-OOK PDM signal transmitter [see Fig. 3(a)], an all-optical regeneration block based on SPM in the nonlinear polarization-diversified fiber loop [see Fig. 3(b)], and a RZ-OOK PDM receiver [see Fig. 3(c)].

In the transmitter, pulses with full-width at half-maximum (FWHM) of 2.3 ps and repetition rate of 10 GHz are first generated using a mode-locked semiconductor laser diode (MLLD), operating at a wavelength of 1556.48 nm. The pulses are then broadened to ∼18 ps by an FBG-type optical filter (OBPF1 with a 3-dB bandwidth of 0.6 nm) and data encoded by a Mach–Zehnder modulator (MZM) with 10-Gb/s$2^{31} - 1$ pseudo random bit sequences (PRBS). The encoded signals are polarization multiplexed to generate 2×10-Gb/s RZ-OOK PDM signals employing a decorrelating scheme that is composed of a coupler, two PCs (PC2 & PC3), a variable optical attenuator (VOA1), 1-km single mode fiber (SMF), and a polarization beam combiner (PBC). Here, two PCs, 1-km SMF and the VOA are used to generate two data streams with orthogonal SOPs, decorrelate two data streams, and balance the optical power between two arms, respectively. We define that the channel with 1-km decorrelating SMF as CH1 and the other as CH2.

The all-optical regeneration block is similar to Fig. 2, and it is composed of an H-EDFA, an ASE rejection filter with 3-dB bandwidth of 0.6 nm (OBPF2), 1-km HNLF, PBS1, a circulator, an IFR with a

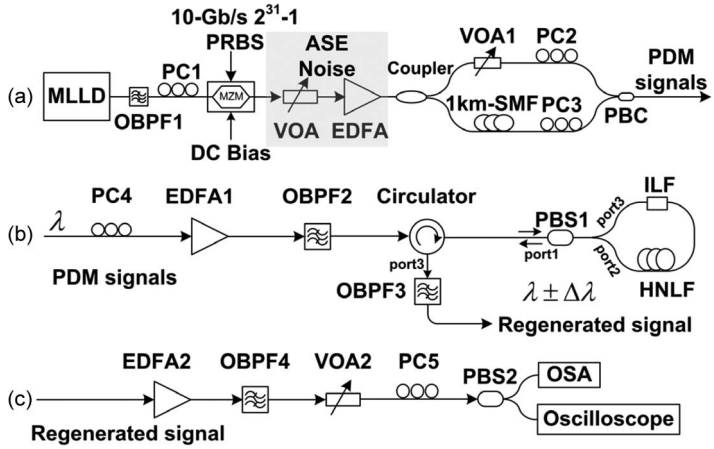

Fig. 3. Experimental setup: (a) 2 × 10-Gb/s RZ-OOK PDM transmitter; (b) all-optical regeneration block; (c) RZ-OOK PDM receiver; MLLD: mode-locked semiconductor laser diode, MZM: Mach–Zehnder modulator, PBC: polarization beam combiner, OSA: optical spectrum analyzer.

round-trip polarization rotation of 90°, and a tunable filter (OBPF3) with 3-dB bandwidth of 0.6 nm. OBPF3 is tunable in both the wavelength and the bandwidth. The zero dispersion wavelength, dispersion slope, and nonlinear coefficient of the HNLF are 1556 nm, 0.02 ps/nm^2/km, and 30 $(\mathrm{W}\cdot\mathrm{km})^{-1}$, respectively. A modified regenerator with improved transfer function is also discussed in Section 4.

At the receiver part, an optical preamplifier (EDFA2), a 0.6-nm filter (OBPF4), a high-speed sampling oscilloscope, and an optical spectrum analyzer (OSA) are used to measure the pulse characteristics after polarization demultiplexing through PC5 and PBS2. The oscilloscope (86100C) has an optical bandwidth of 65-GHz and an electrical bandwidth of 80-GHz. Through the paper, we evaluate the signal performance mainly using the eye-diagram-based signal-to-noise-ratio (SNR) measurement, which is a function provided by the oscilloscope. The optical signal after transmission is directly connected with the optical port of the oscilloscope.

4. Signal Regeneration

4.1. One Section of HNLF

First, we evaluate the performance of simultaneous regeneration of two PDM tributaries following the scheme shown in Fig. 2 (i.e., one section of HNLF with the length of 1-km). RZ-OOK signals are degraded by adjusting the bias of the MZM and adding ASE noise through a booster amplifier (as shown in Fig. 3). The degraded PDM signals are boosted to an optimized average power of ∼20.1 dBm (∼17.1 dBm for each channel) before polarization demultiplexing [PBS1 in Fig. 3(b)]. The offset of OBPF3 in Fig. 3(b) that is used to slice the broadened signals' spectra for regeneration at port3 of the circulator is ∼1.1 nm.

Fig. 4(a) shows the spectra of input degraded and spectrally broadened signals (CH1 and CH2). The difference of broadened spectra between two orthogonal channels is negligible. It indicates that regeneration of two channels simultaneously using only one offset filter (i.e., OBPF3) at the loop's output is feasible.

In addition, Fig. 4(b) compares the spectra of one forward propagating (broadened) signal (CH1), the backscattered noise, and the detuned filter. It can be seen that the power spectral contrast between the broadened forward propagating signal and backscattered noise is up to ∼30 dB near the center wavelength of the offset filter, which indicates that the presence of backscattered noise results in only a slight performance reduction to the counter channel.

Note that in order to achieve an optimized regeneration performance, a step-like transfer function should be obtained to offer the best power equalization, and the broadened spectral components

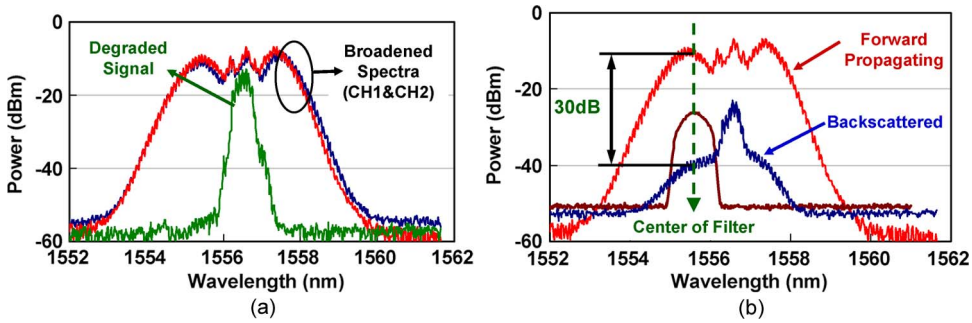

Fig. 4. Measured spectra during PDM regeneration. (a) Spectrum of the degraded signal and broadened spectra of CH1 and CH2. (b) Spectra of forward propagating signal, backscattered signal, and the optical filter.

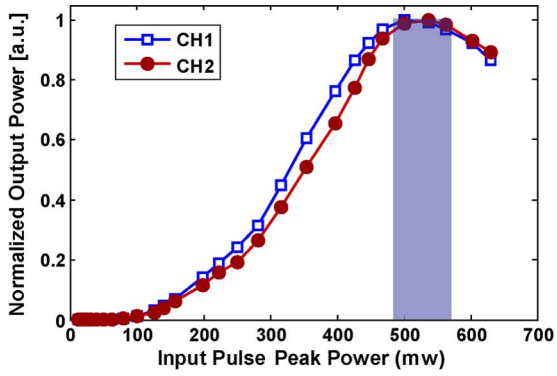

Fig. 5. Transfer functions of the PDM regenerator (input pulse peak power versus normalized output power).

are better to fall into the normal dispersion region for coherence degradation-induced pulse intensity noise and modulation instability suppression [22], [36], [37]. However, due to the low and flat dispersion characteristic of our HNLF, only a non-monotonous type transfer functions (input pulse peak power versus normalized output power) can be obtained for both CH1 and CH2 (as shown in Fig. 5), using only one section of HNLF. Therefore, we use a relative flat operation regime of the transfer function (marked region in Fig. 5), and the offset filter is detuned at the shorter wavelength side (normal dispersion region) for the performance evaluation. The slight difference between CH1 and CH2 is mainly due to the existing 1-km SMF in the PDM transmitter [see Fig. 3(a)].

Fig. 6 shows the measurement results of output (eye-diagram-based) SNR versus input SNR for both PDM channels. All measurements are taken with the same input optical power into the optical port of the oscilloscope (i.e., fixed to -5.0 dBm). Significant improvements are achieved for signals with low input SNR values, e.g., there are $\sim$4.6-dB and 4.8-dB SNR improvements achieved for two PDM signals at the input SNR of $\sim$4.7 dB, respectively. The improvement is limited for input signals with good quality (high SNR). Fluctuation of measurement results mainly come from the sampling oscilloscope itself (although the averaging function is applied). Fig. 7 further shows some typical input and regenerated eye diagrams for comparison. Note that the regenerated pulse streams exhibit slightly amplitude fluctuation at level "1" limited by the non-monotonous type transfer function (i.e., not step-like).

4.2. Optimization of Transfer Function

As previously mentioned, although we achieve the regeneration of PDM signals using the proposed scheme, there is one limitation illustrated in Fig. 5, i.e., a narrow window with flat response.

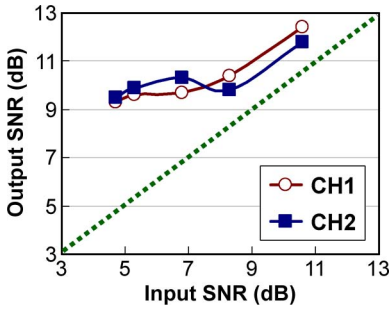

Fig. 6. Measured eye-diagram-based output SNR versus input SNR to show the performance improvements of both PDM channels.

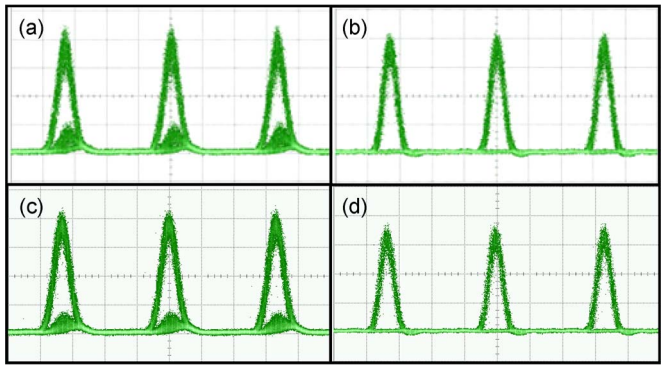

Fig. 7. Typical input and regenerated eye diagrams (only one channel results are shown). (a) Input signal with SNR $\sim$ 4.7 dB and (b) the corresponding regenerated signal with SNR $\sim$ 9.5 dB. (c) input signal with SNR $\sim$ 6.8 dB and (d) the corresponding regenerated signal with SNR $\sim$ 10.3 dB.

Therefore, it would be desired to improve the transfer function through dispersion management [17], [38]. To do that, we use a modified scheme as shown in Fig. 8(a). Instead of using only one section of HNLF, we use two sections of HNLF with similar (almost identical) characteristics (HNLF1 and HNLF2) and add a piece of dispersion-compensating fiber (DCF) in between to reconstruct the regenerator. The lengths of HNLF1, DCF and HNLF2 are 1 km, 200 m, and 1 km, respectively. The dispersion of the 200-m DCF is $\sim$27 ps/nm. Through such a configuration, we improve the transfer function [see Fig. 8(b)].

Based on the modified regenerator, we further evaluate its performance in the same transmission system. Fig. 9 shows the typical spectra during regeneration. Obviously, the broadened spectrum is quite different from that in Fig. 4 in terms of the flatness. The pump power is set to be $\sim$19.6 dBm ($\sim$16.6 dBm for each polarization tributary). Without repeating all the measurements, we set the input SNR to 4.5 dB and measure the output performance as shown in Fig. 10, including the comparison of BER curves between the input (degraded) and output (regenerated) signals with inserted typical eye diagrams. The BER values are taken using MT1810A signal quality analyzer. The performance is further improved ($\sim$1.2 dB) compared with the previous scheme (see Fig. 6).

5. PMD Mitigation

5.1. Single Polarization

PMD mitigation using all-optical regeneration has been demonstrated for a single wavelength channel [39]–[41]. Here, we first confirm the ability of PMD mitigation for a single polarization. Instead using complicated setup shown in Fig. 3, we build another simple setup as shown in Fig. 11(a). It consists of a 10.65-Gbps RZ transmitter, a programmable DGD module as the PMD

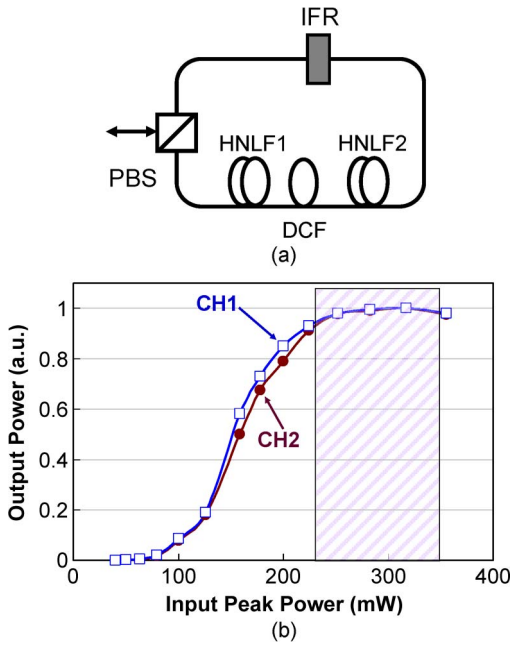

Fig. 8. (a) Modified scheme of the regenerator with improved transfer function and (b) the corresponding transfer function.

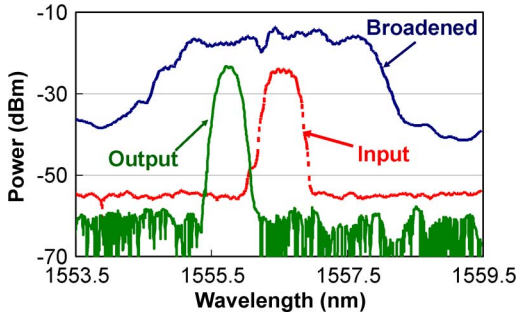

Fig. 9. Spectra of input (degraded), broadened, and output (regenerated).

emulator (PMDE), an SPM-based regenerator, and a receiver. In the transmitter, the light from an external cavity tunable laser (ECL) oscillating at 1555.8 nm is injected into two cascaded MZMs (MOD1 and MOD2) for RZ signal generation (i.e., 50% duty cycle). The regenerator was composed of the H-EDFA, 1-km HNLF, and a tunable OBPF with 3-dB bandwidth of 0.2 nm. After the H-EDFA, the input power to the HNLF is $\sim$23 dBm. The center wavelength of the tunable OBPF is about -0.3 nm shifted from the original signal wavelength. We also evaluate the performance using eye-diagram-based SNR. Fig. 11(b) shows SNR penalty (defined as the difference between the measured SNR under a certain DGD values and without PMD) for both cases, i.e., without regeneration and with regeneration. The maximum SNR improvement as much as 3.7 dB is obtained. Optical regeneration can provide a performance improvement for the DGD value of up to 35 ps. The SNR may be further improved if an ASE noise rejection filter is inserted after the H-EDFA. Note that the SNR only acts as an indicator for comparison; in general, only 2–3 dB Q-penalty happens for 10-Gb/s RZ-OOK signals in the presence of 35-ps PMD. Such simple verification confirms that SPM-based all-optical regeneration can be used for PMD mitigation, which is a motivation for our next demonstration.

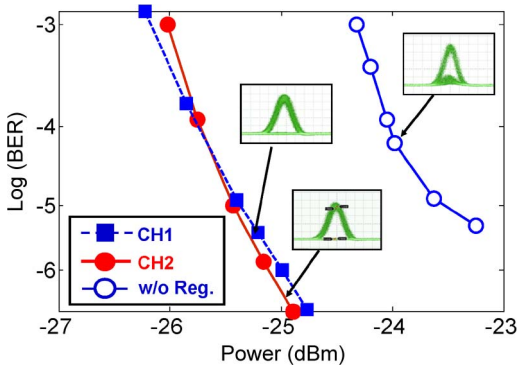

Fig. 10. Comparison of BER curves between the degraded and regenerated signals (CH1 and CH2) with inserted eye diagrams.

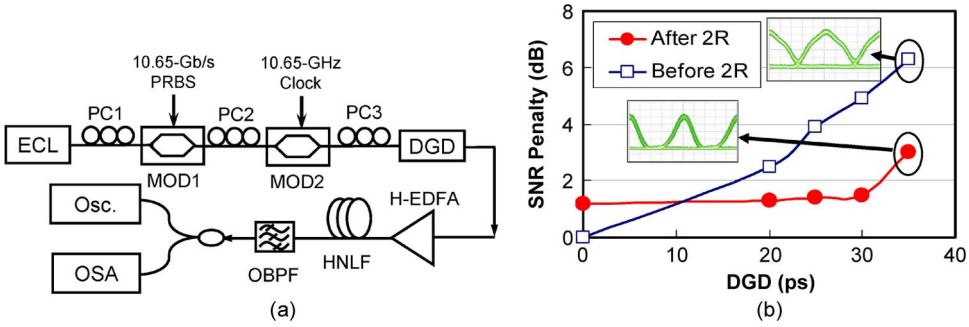

Fig. 11. (a) Experimental setup of PMD mitigation for a single polarization using SPM-based regenerator. (b) Measured SNR variations as a function of DGD for the system with and without the regenerator.

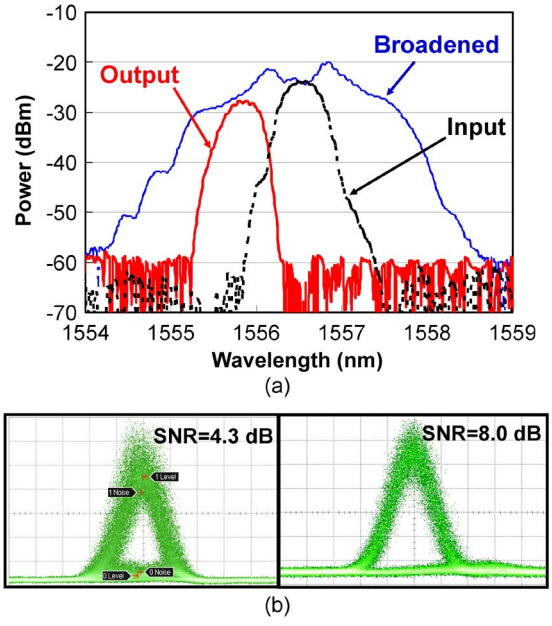

Fig. 12. Results of PMD mitigation. (a) Spectra of degraded signal, broadened signal, and regenerated signal. (b) Comparison of eye diagrams in the presence of 6.3-ps DGD (left: without regeneration; right: with regeneration).

5.2. PDM Signals

We further evaluate the proposed PDM regenerator (modified version) to mitigate PMD effects in PDM systems. A PMDE is inserted at the output of the PDM transmitter [see Fig. 3(a)]. The PMDE consists of a PC and a section of polarization maintaining fiber (PMF) with a certain DGD value. The PMDE is adjusted to emulate the worst case condition, i.e., SOP of the PDM signals is aligned to be 45° with respect to the principle state of polarization (PSP) of the PMDE. Fig. 12(a) shows the spectra of input degraded, spectrally broadened, and regenerated signals. Similar to the case without PMD, only one OBPF (OBPF3) is used for the regeneration. The optical power before PBS1 in Fig. 3(b) is optimized to be ~20.7 dBm (~17.7 dBm for each channel). OBPF3 is detuned ~0.75-nm at port3 of the circulator. Fig. 12(b) shows the comparison of eye diagrams for the DGD value of 6.3-ps (only one polarization). The SNR improvement is ~3.7 dB from 4.3 dB to 8.0 dB.

Several points should be noted: (i) The pulsewidth of RZ-OOK PDM signals is ~18 ps for our experiments, indicating that higher data rate regeneration (e.g. > 40-Gb/s) is feasible (generally, the PMD tolerance exhibits a linear relationship with the pulsewidth of RZ signal). Alternatively, for 10-Gb/s RZ-OOK signals with 50% duty cycle (50-ps pulsewidth), ~17-ps PMD mitigation is achievable for PDM signals. (ii) There is an upper limit of PMD mitigation (e.g., ~8-ps) using all-optical regeneration in our experiment. (iii) We use the manually polarization control to separate the two channels. However, due to possible dramatic polarization perturbations in real applications, dynamic and fast polarization tracking is one of the most challenging techniques in such regenerators [5], [34].

6. Conclusion

In summary, we have proposed and demonstrated an optical regeneration scheme that can work for the PDM signals, even in the presence of a certain amount of PMD. Only one nonlinear module (either one section of HNLF or cascaded sections), one H-EDFA, and one detuned optical filter are required for both PDM channels with orthogonal polarization states. Experimental results at 2 × 10-Gb/s RZ-OOK transmission systems indicate that such a polarization-diversified scheme may be potentially used for other modulation formats as well. However, it is should be noted that the SPM-based cannot improve the signal BER performance at the receiver site once an error occurs, as this regenerator will not be able to correct it [42].

References

[1] A. Gladisch, R. P. Braun, D. Breuer, A. Ehrhardt, H. M. Foisel, M. Jaeger, R. Leppla, M. Schneiders, S. Vorbeck, W. Weiershausen, and F. J. Westphal, "Evolution of terrestrial optical system and core network architecture," *Proc. IEEE*, vol. 94, no. 5, pp. 869–891, May 2006.

[2] M. I. Hayee, M. C. Cardakli, A. B. Sahin, and A. E. Willner, "Doubling of bandwidth utilization using two orthogonal polarizations and power unbalancing in a polarization-division-multiplexing scheme," *IEEE Photon. Technol. Lett.*, vol. 13, no. 8, pp. 881–883, Aug. 2001.

[3] G. Charlet, H. Mardoyan, P. Tran, A. Klekamp, M. Astruc, M. Lefrancois, and S. Bigo, "Upgrade of 10 Gbit/s ultra-long-haul system to 40 Gbit/s with APol RZ-DPSK modulation format," *Electron. Lett.*, vol. 41, no. 22, pp. 1240–1241, Oct. 2005.

[4] J. X. Cai, Y. Cai, C. Davidson, D. Foursa, A. Lucero, O. Sinkin, W. Patterson, A. Pilipetskii, G. Mohs, and N. Bergano, "Transmission of 96× 100 G p re-filtered PDM-RZ-QPSK channels with 300% spectral efficiency over 10 608 km and 400% spectral efficiency over 4,368 km," presented at the Optical Fiber Commun. Conf., San Diego, CA, Mar. 2010, Paper PDPB10.

[5] A. Gnauck, P. J. Winzer, S. Chandrasekhar, X. Liu, B. Zhu, and D. W. Peckham, "10 × 224-Gb/s WDM transmission of 28-Gbaud PDM 16-QAM on a 50-GHz grid over 1,200 Km of fiber," presented at the Optical Fiber Commun. Conf., San Diego, CA, Mar. 2010, Paper PDPB8.

[6] C. Sethumadhavan, X. Liu, B. Zhu, and D. Peckham, "Transmission of a 1.2-Tb/s 24-carrier no-guard-interval coherent OFDM superchannel over 7200-km of ultra-large-area fiber," presented at the Eur. Conf. Optical Commun., Vienna, Austria, Sep. 2009, Paper PD2.6.

[7] K. Croussore, C. Kim, and G. F. Li, "All-optical regeneration of differential phase-shift keying signals based on phase-sensitive amplification," *Opt. Lett.*, vol. 29, no. 20, pp. 2357–2359, Oct. 2004.

[8] K. Croussore and G. Li, "Phase and amplitude regeneration of differential phase-shift keyed signals using phase-sensitive amplification," *IEEE J. Sel. Topics Quantum Electron.*, vol. 14, no. 3, pp. 648–658, May 2008.

[9] J. H. Lee, T. Nagashima, T. Hasegawa, S. Ohara, N. Sugimoto, Y. G. Han, S. B. Lee, and K. Kikuchi, "Output performance investigation of self-phase-modulation-based 2R regenerator using bismuth oxide nonlinear fiber," *IEEE Photon. Technol. Lett.*, vol. 18, no. 12, pp. 1296–1298, Jun. 2006.

[10] N. S. M. Shah and M. Matsumoto, "2R regeneration of time-interleaved multiwavelength signals based on higher order four-wave mixing in a fiber," *IEEE Photon. Technol. Lett.*, vol. 22, no. 1, pp. 27–29, Jan. 2010.
[11] Y. Su, G. Raybon, R. J. Essiambre, and T.-H. Her, "All-optical 2R regeneration of 40-Gb/s signal impaired by intrachannel four-wave mixing," *IEEE Photon. Technol. Lett.*, vol. 15, no. 2, pp. 350–352, Feb. 2003.
[12] M. Matsumoto and Y. Morioka, "Fiber-based all-optical regeneration of DPSK signals degraded by transmission in a fiber," *Opt. Express*, vol. 17, no. 8, pp. 6913–6919, Apr. 2009.
[13] P. V. Mamyshev, "All-optical data regeneration based on self-phase modulation effect," in *Proc. ECOC*, Madrid, Spain, Sep. 1998, vol. 1, pp. 475–476.
[14] M. Matsuura and N. Kishi, "Wideband wavelength-flexible all-optical signal regeneration using gain-band tunable Raman amplification and self-phase-modulation-based spectral filtering," *Opt. Lett.*, vol. 34, no. 16, pp. 2420–2422, Aug. 2009.
[15] N. Yoshikane, I. Morita, and N. Edagawa, "Improvement of dispersion tolerance by SPM-based all-optical reshaping in receiver," *IEEE Photon. Technol. Lett.*, vol. 15, no. 1, pp. 111–113, Jan. 2003.
[16] L. Provost, C. Finot, P. Petropoulos, and J. Richardson, "A 2R Mamyshev regeneration architecture based on a three-fiber arrangement," *J. Lightw. Technol.*, vol. 28, no. 9, pp. 1373–1379, May 2010.
[17] L. Provost, C. Finot, P. Petropoulos, K. Mukasa, and D. J. Richardson, "Design scaling rules for 2R-optical self-phase modulation-based regenerators," *Opt. Express*, vol. 15, no. 8, pp. 5100–5113, Apr. 2007.
[18] A. G. Striegler and B. Schmauss, "Analysis and optimization of SPM-based 2R regeneration at 40 Gb/s," *J. Lightw. Technol.*, vol. 24, no. 7, pp. 2835–2843, Jul. 2006.
[19] M. Matsumoto and O. Leclerc, "Analysis of 2R optical regenerator utilizing self-phase-modulation in highly nonlinear fiber," *Electron. Lett.*, vol. 38, no. 12, pp. 576–577, Jun. 2002.
[20] M. Matsumoto, "Efficient all-optical 2R regeneration using self-phase modulation in bidirectional fiber configuration," *Opt. Express*, vol. 14, no. 23, pp. 11 018–11 023, Nov. 2006.
[21] T. H. Her, G. Raybon, and C. Headley, "Optimization of pulse regeneration at 40 Gb/s based on spectral filtering of self-phase modulation in fiber," *IEEE Photon. Technol. Lett.*, vol. 16, no. 1, pp. 200–202, Jan. 2004.
[22] M. Vasilyev and T. I. Lakoba, "All-optical multichannel 2R regeneration in a fiber-based device," *Opt. Lett.*, vol. 30, no. 12, pp. 1458–1460, Jun. 2005.
[23] C. Kouloumentas, P. Vorreau, L. Provost, P. Petropoulos, W. Freude, J. Leuthold, and I. Tomkos, "All-fiberized dispersion-managed multichannel regeneration at 43 Gb/s," *IEEE Photon. Technol. Lett.*, vol. 20, no. 22, pp. 1854–1856, Nov. 2008.
[24] L. Provost, F. Parmigiani, C. Finot, K. Mukasa, P. Petropoulos, and D. J. Richardson, "Analysis of a two-channel 2R all-optical regenerator based on a counter-propagating configuration," *Opt. Express*, vol. 16, no. 3, pp. 2264–2275, Feb. 2008.
[25] M. Vasilyev, T. I. Lakoba, and P. G. Patki, "Multi-wavelength all-optical regeneration," presented at the Optical Fiber Commun. Conf., San Diego, CA, Feb. 2008, Paper OWK3.
[26] J. Yu, M. F. Huang, and G. K. Chang, "Polarization insensitive wavelength conversion for 4× 112 Gbit/s polarization multiplexing RZ-QPSK signals," *Opt. Express*, vol. 16, no. 26, pp. 21 161–21 169, Dec. 2008.
[27] P. Martelli, P. Boffil, M. Ferrario, L. Marazzi, P. Parolari, R. Siano, V. Pusino, P. Minzioni, I. Cristiani, C. Langrock, M. M. Fejer, M. Martinelli, and V. Degiorgio, "All-optical wavelength conversion of a 100-Gb/s polarization-multiplexed signal," *Opt. Express*, vol. 17, no. 20, pp. 17 758–17 763, Sep. 2009.
[28] J. Lu, L. Chen, Z. Dong, Z. Cao, and S. Wen, "Polarization insensitive wavelength conversion based on orthogonal pump four-wave mixing for polarization multiplexing signal in high-nonlinear fiber," *J. Lightw. Technol.*, vol. 27, no. 24, pp. 5767–5774, Dec. 2009.
[29] A. L. Yi, L. S. Yan, B. Luo, W. Pan, J. Ye, and J. Leuthold, "Self-phase-modulation based all-optical regeneration of PDM signals using a single section of highly nonlinear fiber," *Opt. Express*, vol. 18, no. 7, pp. 7150–7156, Mar. 2010.
[30] L. E. Nelson, T. N. Nielsen, and H. Kogelnik, "Observation of PMD-Induced coherent crosstalk in polarization-multiplexed transmission," *IEEE Photon. Technol. Lett.*, vol. 13, no. 7, pp. 738–740, Jul. 2001.
[31] D. Borne, N. E. Hecker-Denschlag, G. D. Khoe, and H. Waardt, "PMD-induced transmission penalties in polarization-multiplexed transmission," *J. Lightw. Technol.*, vol. 23, no. 12, pp. 4004–4015, Dec. 2005.
[32] Z. Wang, C.-J. Xie, and X. Ren, "PMD and PDL impairments in polarization division multiplexing signals with direct detection," *Opt. Express*, vol. 17, no. 10, pp. 7994–8004, May 2009.
[33] H. Sun, K. T. Wu, and K. Roberts, "Real-time measurements of a 40-Gb/s coherent system," *Opt. Express*, vol. 16, no. 2, pp. 873–879, Jan. 2008.
[34] R. Noé, B. Koch, V. Mirvoda, and D. Sandel, "Endless optical polarization control and PMD compensation," presented at the Optical Fiber Commun. Conf., San Diego, CA, May 2010, Paper OThJ1.
[35] Q. Yang, N. Kaneda, X. Liu, and W. Shieh, "Demonstration of frequency-domain averaging based channel estimation for 40-Gb/s CO-OFDM with high PMD," *IEEE Photon. Technol. Lett.*, vol. 21, no. 20, pp. 1544–1546, Oct. 2009.
[36] N. Nakazawa, H. Kubota, and K. Tamura, "Random evolution and coherence degradation of a high-order optical soliton train in the presence of noise," *Opt. Lett.*, vol. 24, no. 5, pp. 318–320, Mar. 1999.
[37] F. Parmigiani, S. Asimakis, N. Sugimoto, F. Koizumi, P. Petropoulos, and D. J. Richardson, "2R regenerator based on a 2-m-long highly nonlinear bismuth oxide fiber," *Opt. Express*, vol. 14, no. 12, pp. 5038–5044, Jun. 2006.
[38] M. Matsumoto, Y. Shimada, and H. Sakaguchi, "Two-stage SPM-based all-optical 2R regeneration by bidirectional use of a highly nonlinear fiber," *IEEE J. Quantum Electron.*, vol. 45, no. 1, pp. 51–58, Jan. 2009.
[39] B. E. Olsson and D. Blumenthal, "Pulse width restoration and PMD suppression using fiber self-phase modulation," in *Proc. ECOC*, Munich, Germany , 2000, pp. 1–2.
[40] Y. Akasaka, Z. Zhu, Z. Pan, and S. J. Ben Yoo, "PMD mitigation application of MZI-SOA based optical 2R regeneration in the receiver," presented at the Optical Fiber Commun. Conf., Anaheim, CA, Mar. 2005, Paper JWA22.
[41] M. Matsumoto, "Polarization-mode dispersion mitigation by a fiber-based 2R regenerator combined with synchronous modulation," *IEEE Photon. Technol. Lett.*, vol. 16, no. 1, pp. 290–292, Jan. 2004.
[42] M. Rochette, L. Fu, V. Ta'eed, D. J. Moss, and B. J. Eggleton, "2R optical regeneration: An all-optical solution for BER improvement," *J. Lightw. Technol.*, vol. 12, no. 4, pp. 736–744, Aug. 2006.